

Kohta Yamada · Nobuaki Sato · Takeo Fujino  
Choong G. Lee · Isamu Uchida · Jan R. Selman

## Preparation of $\text{LiNiO}_2$ and $\text{LiM}_y\text{Ni}_{1-y}\text{O}_2$ ( $\text{M} = \text{Co,Al}$ ) films by electrostatic spray deposition

Received: 1 April 1998 / Accepted: 23 July 1998

**Abstract** Syntheses of  $\text{LiNiO}_2$ ,  $\text{LiCo}_{0.5}\text{Ni}_{0.5}\text{O}_2$ , and  $\text{LiAl}_{0.25}\text{Ni}_{0.75}\text{O}_2$  as thin films were carried out by electrostatic spray deposition (ESD) onto a gold substrate. Single-phase  $\text{LiNiO}_2$  film was obtained using a precursor solution of  $\text{Li}(\text{OCOCH}_3) + \text{Ni}(\text{OCOCH}_3)_2$ /ethanol, and by heating the deposit at 700 °C under an oxygen stream. In the case of cobalt or aluminum doping,  $\text{Co}(\text{NO}_3)_2$ /ethanol or  $\text{Al}(\text{NO}_3)_3$ /ethanol were added to the precursor solution in a given ratio. X-ray diffractometry revealed that all films had a crystal structure of space group  $R\bar{3}m$ ;  $a = 2.879$ ,  $c = 14.197$  Å for  $\text{LiNiO}_2$ ;  $a = 2.844$ ,  $c = 14.152$  Å for  $\text{LiCo}_{0.5}\text{Ni}_{0.5}\text{O}_2$ ;  $a = 2.855$ ,  $c = 14.148$  Å for  $\text{LiAl}_{0.25}\text{Ni}_{0.75}\text{O}_2$  (in hexagonal setting). Although these products were highly porous, it was observed that the average film thickness of  $\text{LiNiO}_2$  increased almost proportionally with the deposition time. Electrochemical measurements (cyclic voltammetry, charge/discharge measurement at a constant current) were carried out in organic solutions of  $\text{LiClO}_4$  (1 mol  $\text{dm}^{-3}$   $\text{LiClO}_4$ /propylene carbonate + ethylene carbonate). The results indicated that thin films fabricated by ESD were electrochemically active for lithium ion extraction/insertion. The effect of cobalt or aluminum doping on the voltammograms is also described.

**Key words** Electrostatic spray deposition · Thin film · Lithium nickel dioxide cathode · Lithium ion secondary battery

K. Yamada (✉) · N. Sato · T. Fujino  
Institute for Advanced Materials Processing,  
Tohoku University, 2-1-1 Katahira, Aoba-ku,  
Sendai 980-8577, Japan  
e-mail: yamada@ibis.iamp.tohoku.ac.jp  
Tel./Fax: +81-22-2175164

C.G. Lee · I. Uchida  
Department of Applied Chemistry,  
Graduate School of Engineering, Tohoku University,  
Aramaki-Aoba, Aoba-ku, Sendai 980-8579, Japan

J.R. Selman  
Department of Chemical and Environmental Engineering,  
Illinois Institute of Technology, Chicago, IL 60616, USA

### Introduction

The lithium insertion reaction into transition metal oxides forms a class of electrodes with many electrochemical applications. Presently, a large number of lithiation studies are concentrated on cathode materials for secondary lithium ion batteries. Materials reported so far are  $\text{LiCoO}_2$  [1],  $\text{LiMn}_2\text{O}_4$  [2],  $\text{LiNiO}_2$  [3, 4], and those containing dopant [5–8].  $\text{LiMn}_2\text{O}_4$  has a spinel-framework structure and other materials have  $\alpha$ - $\text{NaFeO}_2$ -type structures. Studies of  $\text{LiCoO}_2$  and  $\text{LiMn}_2\text{O}_4$  are more advanced than those of other materials because of the simplicity of preparing these cathodes.

Despite the high cost, the  $\text{LiCoO}_2$  cathode is used in commercial batteries and accepted on the market.  $\text{LiMn}_2\text{O}_4$  is one of the most attractive cathode materials owing to its economic and environmental advantages compared with  $\text{LiCoO}_2$ . However, stoichiometric  $\text{LiMn}_2\text{O}_4$  has been shown to exhibit poor cycling behavior.  $\text{LiNiO}_2$  is also attractive for its electrochemical reactivity in nonaqueous lithium cells. The reactivity strongly depends on the preparation conditions, which affect the structural disorder or defects in the  $\text{LiNiO}_2$  matrix [3]. It is also known that crystal structure changes induced in the cathode by overcharge cause a serious degradation of reversibility in charge/discharge cycles. Although a lot of effort has been made to elucidate the electrochemical properties and the relation between crystal structure and lithium intercalation/deintercalation processes, the investigations have been mainly performed using the pellet-like composite electrodes.

The fabrication of a thin film cathode is an important requirement for a thin layer-type high-energy-density battery. In such thin films the inserted lithium ions diffuse across a short distance, and a quasi-equilibrium charge/discharge is attained in a shorter time compared to pellet-type electrodes. In addition, the thin film technique allows examination of the electrochemically interesting behavior of the cathode simultaneously with the crystallographic properties. For example, in situ

conductivity-potential profiles can be obtained by using thin film electrodes combined with interdigitated microarray electrodes [9]. To do this, one must optimize the available ways to prepare thin film cathodes.

LiCoO<sub>2</sub> and LiMn<sub>2</sub>O<sub>4</sub> thin films have been synthesized by several methods: radiofrequency sputtering [10, 11], laser ablation [12], chemical vapor deposition [13], or electrostatic spray deposition (ESD) [14–16]. However, attempts to prepare LiNiO<sub>2</sub> thin films have not been reported. This may be due to the difficulty of fabricating an electrochemically active LiNiO<sub>2</sub> thin film. In the present study we carried out the synthesis of LiNiO<sub>2</sub> in thin film form by ESD and investigated its electrochemical properties in an organic solution. The effect of doping the LiNiO<sub>2</sub> thin film with cobalt or aluminum was also examined. These are attractive elements because LiNiO<sub>2</sub>, LiCoO<sub>2</sub>, and  $\alpha$ -LiAlO<sub>2</sub> are isostructural with  $\alpha$ -NaFeO<sub>2</sub>, having a space group  $R\bar{3}m$  in which transition metal and alkali metal ions are respectively located at 3a and 3b sites in a cubic close-packed oxygen array.

## Experimental

The principle of the ESD technique is schematically shown in Fig. 1 [14–17]. This method comprises generating an aerosol by applying a high voltage between a substrate and a sprayed solution containing the desired precursor materials. In the set-up used here the solution was sprayed downward to a substrate.

All chemicals were of reagent grade and used as received. As precursor materials, Li(OCOCH<sub>3</sub>)<sub>2</sub>·2H<sub>2</sub>O, Ni(OCOCH<sub>3</sub>)<sub>2</sub>·4H<sub>2</sub>O, Co(NO<sub>3</sub>)<sub>2</sub>·6H<sub>2</sub>O, and Al(NO<sub>3</sub>)<sub>3</sub>·9H<sub>2</sub>O (Wako Pure Chemicals) were used. The stock solutions of these reagents were ethanol solutions of 0.055 mol dm<sup>-3</sup> of Li(OCOCH<sub>3</sub>)<sub>2</sub>·2H<sub>2</sub>O and 0.050 mol dm<sup>-3</sup> of the others. The solutions were well mixed in a given molar ratio (Li/Ni = 1.1/1, Li/Ni/Co = 1.1/0.5/0.5, Li/Ni/Al = 1.1/0.75/0.25) as a precursor solution prior to each experiment. The ratio of lithium to nickel or summation of nickel and dopant metals was higher than the stoichiometric ratio to avoid lithium deficiency. The concentration of lithium in precursor solutions was 0.0275 mol dm<sup>-3</sup>, and that of nickel or mixtures of Ni/Co or Ni/Al was 0.025 mol dm<sup>-3</sup>.

In this study a gold flag-type disk electrode (Nilaco, 99.95%, 6 mm diameter, 0.1 mm thick) was used as a substrate to avoid interaction with lithium ions under oxidizing conditions and to simplify identification of the product. The substrate was put on a

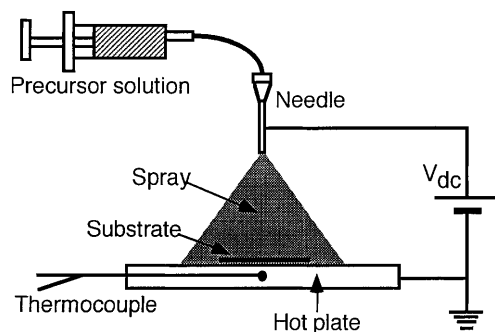


Fig. 1 Schematic representation of the electrostatic spray deposition (ESD) technique

hot plate made of aluminum (15 × 15 × 1.5 cm) with three seamless heaters (Firerod, 500 W type), and grounded via the plate. The temperature of the hot plate was monitored by a Alumel-Chromel-type thermocouple sheathed in a stainless steel tube, and controlled at 350 ± 5 °C. The precursor solutions flowed through a stainless needle (0.3 mm I.D., 0.5 mm O.D., 22 mm length) using a syringe pump (Kd Scientific type 100) at a rate of 3.9 ml h<sup>-1</sup>. A 20 ml glass syringe (18 mm I.D.) was used. A Teflon tube was used to connect the syringe and the needle.

To generate an aerosol of precursor materials, a positive voltage of 11 kV was applied to the needle using a high-voltage power supply (Matsusada Precision, type HVR-12P) with a flowing precursor solution. The needle-substrate distance was fixed at 5.5 cm. These values were determined from the viewpoint of homogeneity of spraying, and fixed through experiments. The deposition was conducted for 1–6 h, and both sides of the substrate were covered for the same deposition time. To measure film thickness, a gold substrate partly covered with an aluminum sheet was sprayed to distinguish a step.

The sample deposited on the substrate by spraying was calcined in an alumina boat at 450 °C for 0.5 h under air, and successively heated at 700 °C for 1.5 h under an oxygen stream. The product, cooled with flowing oxygen, was immediately transferred to a vacuum vessel, where it was kept to avoid exposure to moisture until the electrochemical measurements were made. The amount of product was determined using a highly sensitive electromicrobalance (Mettler, MT5). Normally, the amount was in the range of 0.1–0.7 mg. The compositions of dopant and nickel were determined using an electron probe X-ray microanalyser (EPMA) (Hitachi, X-650S).

The phase of the product was identified by X-ray diffractometry (XRD) (Rigaku, RAD-IC diffractometer). CuK $\alpha$ <sub>1</sub> ( $\lambda = 1.54056$  Å) radiation (40 kV, 20 mA) monochromatized with curved pyrolytic graphite was used. The slit system was 1°–1°–0.15–0.3 mm. The scanning speed was 1°/min<sup>-1</sup>. The data were collected at 0.02° intervals. The intensity and least-squares lattice parameter calculations were carried out with the LAZY-PULVERIX [18] and LCR2 [19] programs, respectively.

The morphology of the product was observed by a scanning electron microscope (Hitachi, S-4100L). The average film thickness was determined by a surface profile measuring system (Ulvac DekTak<sup>3</sup>ST).

Electrochemical measurements were performed in a mixture of propylene carbonate (PC) and ethylene carbonate (EC) containing 1 mol dm<sup>-3</sup> LiClO<sub>4</sub> in a dry box filled with dry air. A T-type glass cell was assembled in a glove box filled with argon gas. The reference and the counter electrodes were lithium foil sustained by nickel mesh metal. Cyclic voltammetry was carried out using a potentiostat (Hokuto, HAB151) controlled by a personal computer combined with an AD/DA converter (Adtek, System Science, type AB98-57B) and a custom-made program. The upper and lower potential limits were set at 4.3 V and 3.0 V, respectively, and the potential scanning rate was 0.3 mV s<sup>-1</sup>. The charge/discharge test at a constant current of 17  $\mu$ A cm<sup>-2</sup> was carried out using a Mac Pile system (CNRS Science Instruments). The potential limits were 4.3 V and 3.3 V. In both cases, the measurements were repeated for five cycles.

## Results and discussion

### LiNiO<sub>2</sub> film

Figure 2 shows a typical XRD pattern of LiNiO<sub>2</sub> film deposited for 6 h (average film thickness: 10.3  $\mu$ m). In the figure the peaks of the gold substrate are also shown. The halo pattern between 15° and 35° was attributed to the glass holder used to sustain the 6 mm diameter gold substrate with products. All the peaks except those of the substrate can be assigned to the  $\alpha$ -NaFeO<sub>2</sub>-type

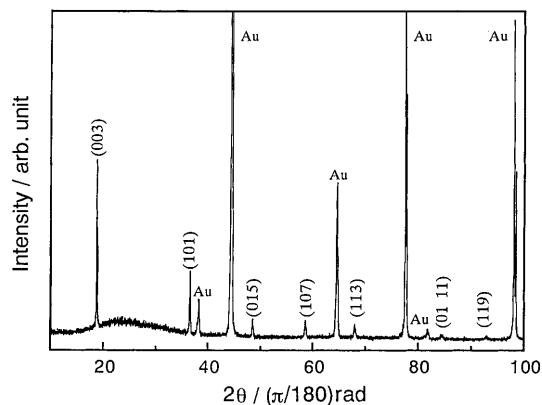


Fig. 2 X-ray diffraction (XRD) pattern of LiNiO<sub>2</sub> film synthesized by ESD. Deposition time was 6 h

crystal structure of space group  $R\bar{3}m$ , indicating that the product was a single phase. The lattice parameters of LiNiO<sub>2</sub> were calculated by the Nelson-Riley least-squares method on the LCR2 program and found to be  $a = 2.879$ ,  $c = 14.197$  Å in hexagonal setting. These values were slightly different from the reported values ( $a = 2.88$ ,  $c = 14.18$  Å) [4]. This may be attributed to the difference in preparation conditions. It is generally accepted that the deviation from the stoichiometric ratio of Li/Ni can be estimated from the ratio of the integrated intensity of  $I(003)/I(104)$  [20]. However, this XRD result could not be used for such an estimate owing to overlapping of the (104) reflection and a strong substrate peak. Although in macroscopic observation the surface morphology of the LiNiO<sub>2</sub> film exhibited the appearance of a smooth film, close observation by scanning electron microscopy suggested that the films were quite porous. In spite of this highly porous appearance in close-up, it was found that a linear relation exists between the average film thickness and the deposition time, as shown in Fig. 3. The film growth rate was about  $1.6 \mu\text{m h}^{-1}$ .

From XRD it was concluded that the thin film thus prepared was a single-phase LiNiO<sub>2</sub>. Figure 4 shows

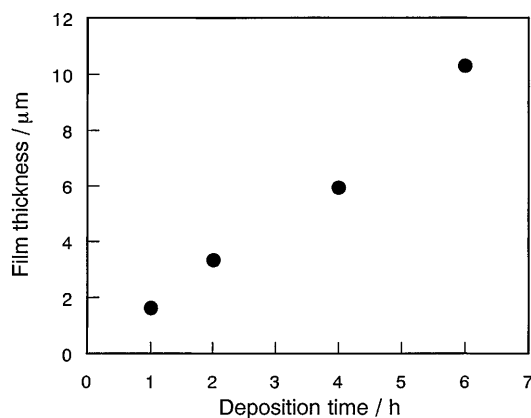


Fig. 3 Dependence of deposition time on LiNiO<sub>2</sub> film thickness

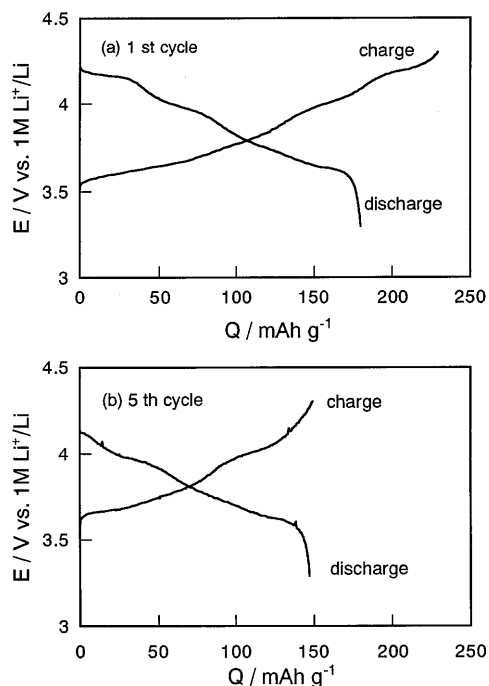
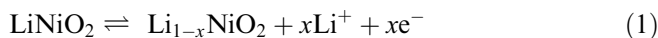


Fig. 4a, b Charge/discharge curves for a LiNiO<sub>2</sub> film electrode at a constant current of  $17 \mu\text{A cm}^{-2}$  in  $1 \text{ mol dm}^{-3}$  LiClO<sub>4</sub>/(PC + EC). The deposition time was 4 h. a first cycle, b fifth cycle

typical charge/discharge curves for a LiNiO<sub>2</sub> film deposited for 4 h. It is noteworthy that exposure of the electrode to moisture should be prevented in order to maintain the charge/discharge capability constant. Moisturizing the film resulted in performance degradation. The open circuit voltage of a freshly prepared film was around 3.3 V. Upon charging, the initial charge capacity until the cut-off voltage of 4.3 V was ca.  $230 \text{ mAh g}^{-1}$  based on LiNiO<sub>2</sub> sample weight. With this charge capacity, the  $x$  value in Li<sub>1-x</sub>NiO<sub>2</sub> of the following equation was calculated to be 0.84 at the end of charging:



The initial discharge capacity was smaller than the charging capacity by  $49 \text{ mAh g}^{-1}$ , so the coulombic efficiency (discharge capacity/charge capacity) was 79%. However, it increased to 99% by the fifth cycle, and the  $x$  value at the end of charge was 0.54. Although some ambiguities remain about the initial large capacity loss, we have confirmed the coulombic reversibility during charge/discharge cycling for this thin film.

In Fig. 4, several plateaus can be distinguished. In order to clarify the potential profile of this redox behavior,  $dQ/dE$  for the fifth cycle was plotted against  $E$  in Fig. 5. During charging, two main peaks at 3.66 V and 4.00 V are observed, and the corresponding peaks during discharging are at 3.62 V and 3.97 V. The mid-point potentials for these redox peaks were calculated to be 3.64 V and 3.99 V. These results are similar to the behavior reported for a pellet-type LiNiO<sub>2</sub> electrode [4].

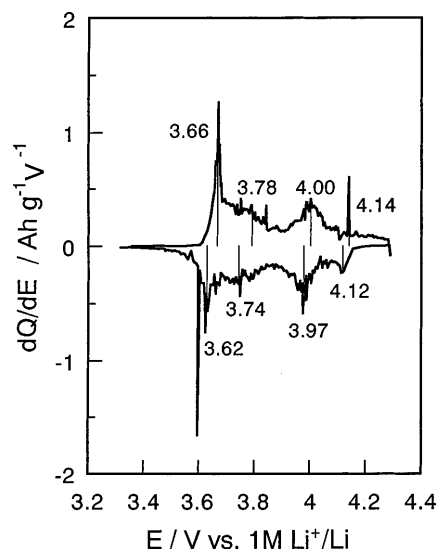


Fig. 5  $dQ/dE$  versus  $E$  plot from the charge/discharge curve of Fig. 4

XRD analysis at open circuit potential (3.3 V) and at the cut-off potential (4.3 V), as shown in Fig. 6, was used to observe the structure change. The  $2\theta$  angle of the (003) reflection shifted to a lower value during charging from 3.3 V to 4.3 V, while the angles of the (101) and (113) reflections shifted to higher values. This observation agrees with results in the literature [21]. The XRD pattern at 4.3 V may be assigned to the crystal structure  $R\bar{3}m$ , in which case the lattice parameters at 4.3 V were  $a = 2.841$ ,  $c = 14.323$  Å (in hexagonal setting). The volume change of the unit cell decreased by 2%. From the results described above, it may be concluded that the  $\text{LiNiO}_2$  film prepared by ESD is electrochemically the same as that of samples prepared in other ways [4, 21].

To investigate the doping effect of cobalt or aluminum, comparative cyclic voltammetry studies were carried out for doped and non-doped  $\text{LiNiO}_2$  films. Figure 7 shows cyclic voltammograms for non-doped  $\text{LiNiO}_2$  film in  $1 \text{ mol dm}^{-3} \text{ LiClO}_4/(\text{PC} + \text{EC})$  at a scan rate  $0.3 \text{ mV s}^{-1}$ . A single broad peak at  $E_p^a = 3.85 \text{ V}$  was observed during the anodic scan, with corresponding cathodic peaks at  $E_p^c = 3.45 \text{ V}$ . It was found that the peak potential hardly changed upon repeated cycling up

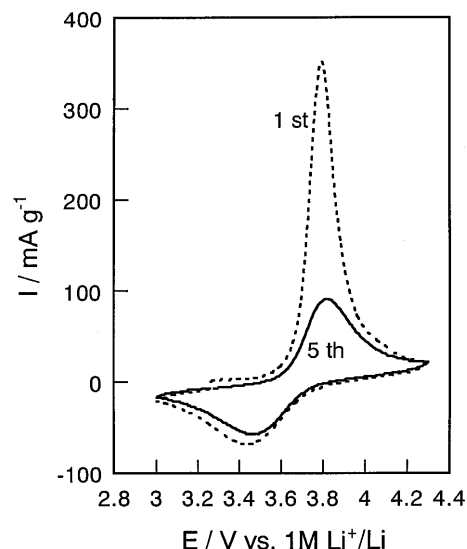


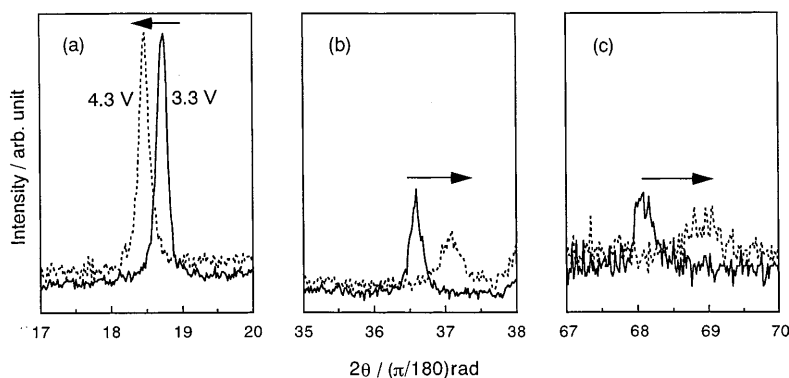
Fig. 7 Cyclic voltammograms for a  $\text{LiNiO}_2$  film electrode in  $1 \text{ mol dm}^{-3} \text{ LiClO}_4/(\text{PC} + \text{EC})$  at a scan rate  $0.3 \text{ mV s}^{-1}$ . The deposition time was 1 h

to the fifth scan. The peak separation was 0.4 V, and the mid-point voltage was calculated to be 3.65 V. The observed voltammograms correspond very well to the potential profile of  $dQ/dE$  shown in Fig. 5.

#### Co-doped $\text{LiNiO}_2$ film

Figure 8 shows the XRD pattern of  $\text{LiCo}_{0.5}\text{Ni}_{0.5}\text{O}_2$  film of deposition time 4 h. The ratio of Co/Ni determined by the EPMA technique was 47/53. All the peaks except those of the substrate can be explained by the crystal structure  $R\bar{3}m$ . It is clear that the product is a single phase. The calculated lattice parameters were  $a = 2.844$ ,  $c = 14.152$  Å (in hexagonal setting), and these values are close to the values of  $a = 2.84$ ,  $c = 14.1$  Å reported in the literature [5]. The cell volume changed by doping with cobalt, the unit cell volume being reduced by 3%, which is close to the result in the literature [5]. Since the lattice parameter changes, the (104) reflection peak becomes distinguishable from the substrate peak.

Fig. 6a–c Shift of XRD peak over the potential change from 3.3 V to 4.3 V. **a** (003), **b** (101), **c** (113) reflections



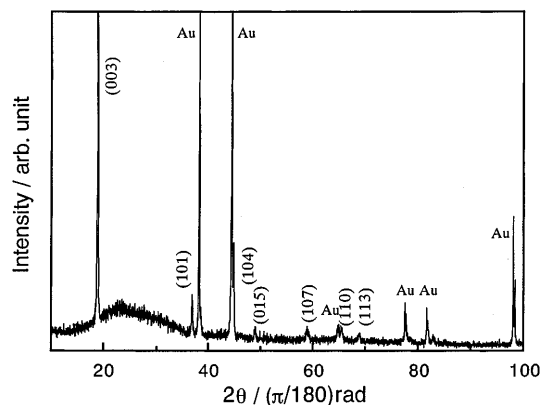


**Fig. 8** XRD pattern of  $\text{LiCo}_{0.5}\text{Ni}_{0.5}\text{O}_2$  film synthesized by ESD. Deposition time was 4 h

Figure 9 shows cyclic voltammograms for  $\text{LiCo}_{0.5}\text{Ni}_{0.5}\text{O}_2$  film obtained under the same conditions as Fig. 7. Surprisingly, the peak at 3.54 V during the initial anodic scan was smaller than others. In the cycles following the initial scan, two peaks were observed at  $E_p^a = 3.60$  V and 3.67 V, with a corresponding peak at 3.54 V and a small shoulder at 3.65 V during the cathodic scan. Although with cycling the anodic peak potentials shifted slightly positive, the peak separations between the anodic and cathodic peaks were much smaller than those in Fig. 7. The charge/discharge coulombic efficiency in the fifth cycle was 94%. These results lead to the conclusion that the charge/discharge behavior of  $\text{LiCo}_{0.5}\text{Ni}_{0.5}\text{O}_2$  was improved compared with that of  $\text{LiNiO}_2$ .

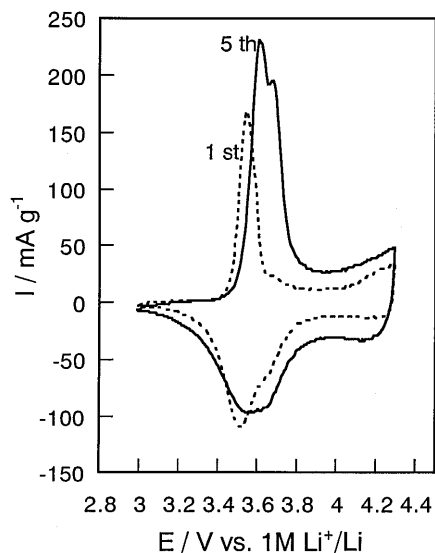
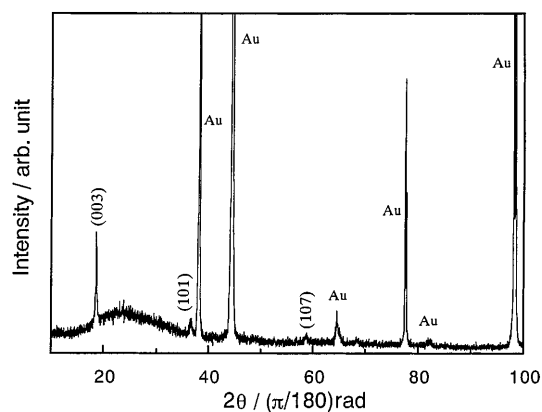


**Fig. 9** Cyclic voltammograms for a  $\text{LiCo}_{0.5}\text{Ni}_{0.5}\text{O}_2$  film electrode in  $1 \text{ mol dm}^{-3} \text{ LiClO}_4/(\text{PC}+\text{EC})$  at a scan rate  $0.3 \text{ mV s}^{-1}$ . The deposition time was 1 h

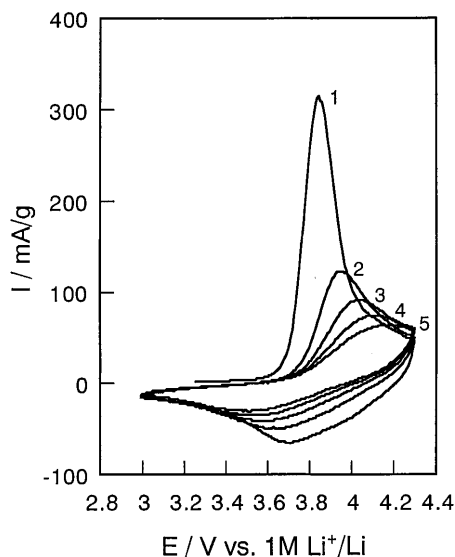
### Al-doped $\text{LiNiO}_2$ film

Figure 10 shows the XRD pattern of a  $\text{LiAl}_{0.25}\text{Ni}_{0.75}\text{O}_2$  film of deposition time 4 h. The ratio of Al/Ni determined by the EPMA technique was 21/79. In this figure the peak intensities of the film product were weak and the peaks were ambiguous. Although it is necessary to anneal at a higher temperature in order to improve the crystallinity of the product, in the case of the synthesis using the open system the deficiency of alkali metal in the product is frequently observed after annealing at high temperature. In the present experiment, since it was observed that the peak intensity of the (003) reflection gradually reduced with increasing reaction time at  $750^\circ\text{C}$ , the annealing was carried out at  $700^\circ\text{C}$ . Although the intensities of the peaks in Fig. 10 were weak, all peaks except those of the substrate could be assigned to the  $R\bar{3}m$  structure, indicating that the product was a single phase. The lattice parameters of  $\text{LiAl}_{0.25}\text{Ni}_{0.75}\text{O}_2$  were calculated to be  $a = 2.855$ ,  $c = 14.148 \text{ \AA}$ . These values were slightly different from the reported values ( $a = 2.86$ ,  $c = 14.24 \text{ \AA}$ ) [6].

Figure 11 shows cyclic voltammograms for a  $\text{LiAl}_{0.25}\text{Ni}_{0.75}\text{O}_2$  film under the same conditions as Fig. 7; in the first cycle,  $E_p^a = 3.84$  V for the anodic scan and  $E_p^c = 3.70$  V for the cathodic scan. However, the peak separation rapidly became broader with cycling. The charge/discharge coulombic efficiency in the fifth cycle was 62%. Apparently the doping of  $\text{LiNiO}_2$  with aluminum resulted in considerable degradation of the charge/discharge behavior. The increased peak separation might be attributed to the irreversible change of crystal structure and/or the iR contribution: aluminum doping may cause the reduction of electronic conductivity. To clarify the iR contribution, more detailed investigations are needed that focus on in situ measurements like the conductivity-potential profiles [9].



**Fig. 10** XRD pattern of a  $\text{LiAl}_{0.25}\text{Ni}_{0.75}\text{O}_2$  film synthesized by ESD. Deposition time was 4 h



**Fig. 11** Cyclic voltammograms for a  $\text{LiAl}_{0.25}\text{Ni}_{0.75}\text{O}_2$  film electrode in  $1 \text{ mol dm}^{-3} \text{ LiClO}_4/(\text{PC} + \text{EC})$  at a scan rate  $0.3 \text{ mV s}^{-1}$ . The deposition time was 1 h. The cycle numbers are shown in figure

## Conclusions

Thin films of  $\text{LiNiO}_2$ ,  $\text{LiCo}_{0.5}\text{Ni}_{0.5}\text{O}_2$ , and  $\text{LiAl}_{0.25}\text{Ni}_{0.75}\text{O}_2$  were synthesized on a gold substrate by ESD. XRD revealed that each film was a single phase, and had the  $R\bar{3}m$  crystal structure. The lattice parameters calculated using the LCR2 program were  $a = 2.879$ ,  $c = 14.197 \text{ \AA}$  for  $\text{LiNiO}_2$ ;  $a = 2.844$ ,  $c = 14.152 \text{ \AA}$  for  $\text{LiCo}_{0.5}\text{Ni}_{0.5}\text{O}_2$ ; and  $a = 2.855$ ,  $c = 14.148 \text{ \AA}$  for  $\text{LiAl}_{0.25}\text{Ni}_{0.75}\text{O}_2$  (in hexagonal setting). All of these films were porous, and the average film thickness of  $\text{LiNiO}_2$  increased almost linearly with the deposition time. Electrochemical characterization was carried out by cyclic voltammetry and charge-discharge tests. These tests revealed that all of the thin films were electro-

chemically active for lithium ion extraction/insertion in  $1 \text{ mol dm}^{-3} \text{ LiClO}_4/(\text{PC} + \text{EC})$ . While cobalt doping of the  $\text{LiNiO}_2$  film improved the charge/discharge behavior, aluminum doping resulted in its degradation.

## References

- Mizushima K, Jones PC, Wiseman PC, Goodnough JB (1980) *Mater Res Bull* 15: 783
- Shokoohi FK, Tarascon JM, Wilkens BJ, Guyomard D, Chang CC (1992) *J Electrochem Soc* 139: 1845
- Dahn JR, Sacken U, Michal CA (1990) *Solid State Ionics* 44: 87
- Ohzuku T, Ueda A, Nagayama M (1993) *J Electrochem Soc* 140: 1862
- Ueda A, Ohzuku T (1994) *J Electrochem Soc* 141: 2010
- Ohzuku T, Ueda A, Kouguchi M (1995) *J Electrochem Soc* 142: 4033
- Sanchez L, Tirado JL (1997) *J Electrochem Soc* 144: 1939
- Zhong Q, Bonakdarpour A, Zhang M, Gao Y, Dahn JR (1997) *J Electrochem Soc* 144: 205
- Shibuya M, Nishina T, Matsue T, Uchida I (1996) *J Electrochem Soc* 143: 3157
- Birke P, Chu WF, Weppner W (1996) *Solid State Ionics* 93: 1
- Thackerray MM (1997) *J Electrochem Soc* 144: L100
- Antaya M, Dahn JR, Preston JS, Rossen E, Reimers JN (1993) *J Electrochem Soc* 140: 575
- Fragnaud P, Nagarajan R, Schleich DM, Vujic D (1995) *J Power Sources* 54: 175
- Chen C, Buysman AAJ, Kelder EM, Schoonman J (1995) *Solid State Ionics* 80: 1
- Chen C, Kelder EM, van der Put PJJM, Schoonman J (1996) *J Mater Chem* 6: 765
- van Zomeren AA, Kelder EM, Marijnissen JCM, Schoonman J (1994) *J Aerosol Sci* 25: 1229
- Kelder EM, Nijs OCJ, Schoonman J (1994) *Solid State Ionics* 68: 5
- Yvon K, Jeitschko W, Parthe E (1977) *J Appl Crystallogr* 10: 73
- Williams DE (1964) Ames Lab Report IS-1052
- Morales J, Perez-Vicente C, Tirado JL (1990) *Mat Res Bull* 25: 623
- Li W, Reimers JN, Dahn JR (1993) *Solid State Ionics* 67: 123